Article

Structure–Property Correlations in Polypropylene from Metallocene Catalysts: Stereodefective, Regioregular Isotactic Polypropylene

Claudio De Rosa, Finizia Auriemma, Annunziata Di Capua, Luigi Resconi, Simona Guidotti, Isabella Camurati, Ilya E. Nifant'ev, and Ilya P. Laishevtsev

J. Am. Chem. Soc., **2004**, 126 (51), 17040-17049• DOI: 10.1021/ja045684f • Publication Date (Web): 02 December 2004

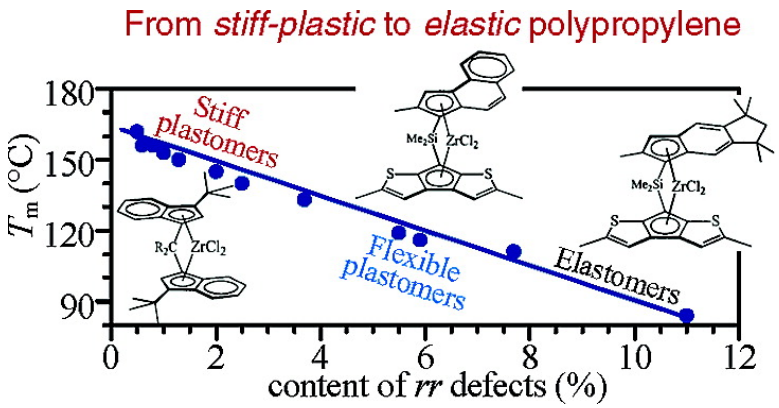

More About This Article

Additional resources and features associated with this article are available within the HTML version:

- Supporting Information
- Links to the 9 articles that cite this article, as of the time of this article download
- Access to high resolution figures
- Links to articles and content related to this article
- Copyright permission to reproduce figures and/or text from this article

View the Full Text HTML

J|A|C|S
ARTICLES
Published on Web 12/02/2004

Structure−Property Correlations in Polypropylene from Metallocene Catalysts: Stereodefective, Regioregular Isotactic Polypropylene

Claudio De Rosa,*,† Finizia Auriemma,† Annunziata Di Capua,† Luigi Resconi,*,‡ Simona Guidotti,‡ Isabella Camurati,‡ Ilya E. Nifant'ev,§ and Ilya P. Laishevtsev§

Contribution from the Dipartimento di Chimica, Università di Napoli "Federico II", Complesso Monte S. Angelo, Via Cintia, 80126 Napoli, Italy, Basell Polyolefins, Centro Ricerche G. Natta, P.le G. Donegani 12, I-44100 Ferrara, Italy, and Chemistry Department, M. V. Lomonosov Moscow State University, Moscow, Russia 119899

Received July 19, 2004; E-mail: claudio.derosa@unina.it; luigi.resconi@basell.it

Abstract: A series of MAO-activated C_1-symmetric indenyl-*ansa*-dithienocyclopentadienyl-based zirconocenes have been used to produce isotactic polypropylenes of medium to high molecular weights, of different degrees of stereoregularity, and free from regioerrors. The effect of the presence of *rr* defects on the polymorphic behavior and mechanical properties of polypropylene is analyzed. The presence of *rr* defects induces crystallization of γ form and of disordered modifications intermediate between α and γ forms. A linear relationship between the amount of γ form and the average length of isotactic sequences has been found. Samples with low concentration of *rr* defects, up to 3−4%, present high melting temperatures, in the range 160−130 °C, and behave as stiff-plastic materials; sample with higher *rr* content, in the range 4−6% and melting temperatures around 115−120 °C are highly flexible thermoplastic materials, and, finally, samples with concentration of *rr* defects in the range 7−11% and melting temperatures in the range 80−110 °C are thermoplastic elastomers with high strength. The fine-tuning of the chain microstructure, achieved by a tailored design of new metallocene catalysts, has allowed production of new polypropylenes having desired properties, intermediate between those of stiff plastic and elastomeric materials.

Introduction

Single-center catalysts allow the production of polypropylenes (PP) of virtually any microstructure.[1,2] The microstructure and the molecular weight of PP in turn determine the crystallization behavior and its physical properties.[3−8] Among the most isospecific metallocenes, two classes are worth mentioning here: those of general structure *rac*-Me_2Si(2-Methyl-4-Aryl-indenyl)$_2ZrCl_2$, which produce polypropylenes of very high isotacticities (*mmmm* ≥ 99%) and molecular weights with melting points as high as 160 °C,[9] but not fully regioselective (showing 0.5−1% of isolated erythro 2,1 units), and the less stereoselective, but fully regioselective, complexes of structure *rac*-R_2C(3-*tert*-butylindenyl)$_2ZrCl_2$.[10,11] The two examples of the latter family, relevant to the present investigation, are shown in Chart 1.

Chart 1. Structure of the C_2-Symmetric *ansa*-Zirconocenes of the Present Study[a]

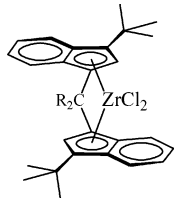

[a] **1**: R = H. **2**: R = CH_3

Some of us have recently described the use of C_1-symmetric *ansa*-zirconocenes, which are characterized by the (substituted indenyl)-dimethylsilyl-[bis(2-methylthieno)cyclopentadienyl]

† Università di Napoli "Federico II".
‡ Basell Polyolefins.
§ M. V. Lomonosov Moscow State University.

(1) Resconi, L.; Cavallo, L.; Fait, A.; Piemontesi, F. *Chem. Rev.* **2000**, *100*, 1253.
(2) Resconi, L. In *Synthesis of atactic polypropylene using metallocene catalysts*; Kaminsky, W., Scheirs, J., Ed.; Wiley: New York, 1999; Vol. 1, p 467.
(3) Auriemma, F.; De Rosa, C.; Boscato, T.; Corradini, P. *Macromolecules* **2001**, *34*, 4815. De Rosa, C.; Auriemma, F.; Perretta, C. *Macromolecules* **2004**, *37*, 6843.
(4) De Rosa, C.; Auriemma, F.; Circelli, T.; Waymouth, R. M. *Macromolecules* **2002**, *35*, 3622
(5) Auriemma, F.; De Rosa, C. *Macromolecules* **2002**, *35*, 9057.
(6) De Rosa, C.; Auriemma, F.; Circelli, T.; Longo, P.; Boccia, A. C. *Macromolecules* **2003**, *36*, 3465.
(7) De Rosa, C.; Auriemma, F.; Spera, C.; Talarico, G.; Tarallo, O. *Macromolecules* **2004**, *37*, 1441.
(8) De Rosa, C.; Auriemma, F.; Ruiz de Ballesteros, O.; Resconi, L.; Fait, A.; Ciaccia, E.; Camurati, I. *J. Am. Chem. Soc.* **2003**, *125*, 10913. De Rosa, C.; Auriemma, F.; Ruiz de Ballesteros, O. *Macromolecules* **2003**, *36*, 7607. De Rosa, C.; Auriemma, F.; Ruiz de Ballesteros, O. *Macromolecules* **2004**, *37*, 1422. Auriemma, F.; De Rosa, C. *J. Am. Chem. Soc.* **2003**, *125*, 13143.
(9) Spaleck, W.; Küber, F.; Winter, A.; Rohrmann, J.; Bachmann, B.; Antberg, M.; Dolle, V.; Paulus, E. *Organometallics* **1994**, *13*, 954.
(10) Resconi, L.; Piemontesi, F.; Camurati, I.; Sudmeijer, O.; Nifant'ev, I. E.; Ivchenko, P. V.; Kuz'mina, L. G. *J. Am. Chem. Soc.* **1998**, *120*, 2308.
(11) Resconi, L.; Balboni, D.; Baruzzi, G.; Fiori, C.; Guidotti, S. *Organometallics* **2000**, *19*, 420.

10.1021/ja045684f CCC: $27.50

Chart 2. Structures of the C_1-Symmetric Zirconocene Precatalysts **3**−**10**

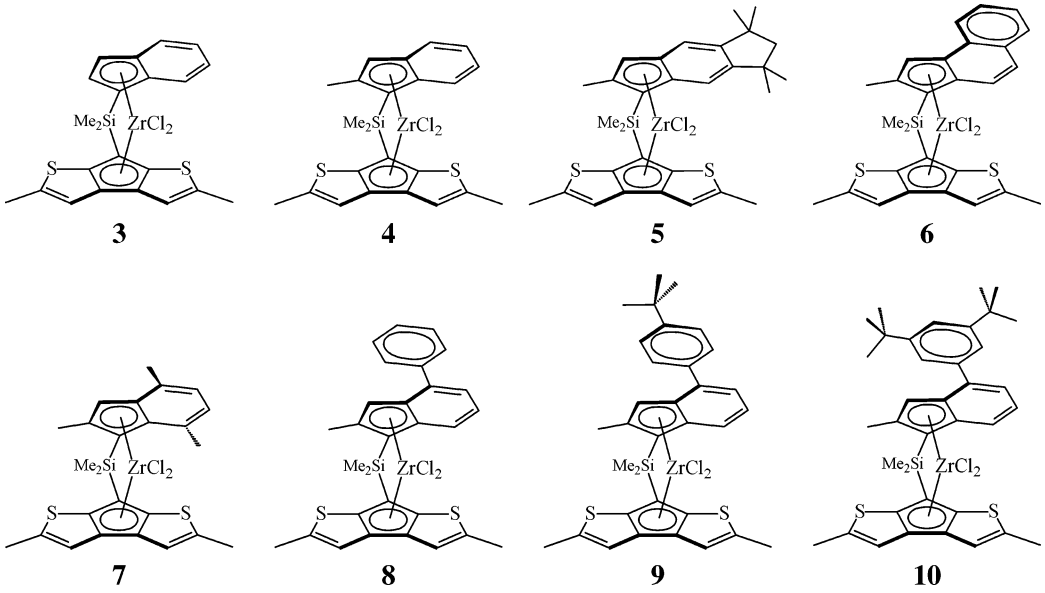

Table 1. Polymerization Temperatures (T_p), Viscosity Average Molecular Masses (M_v), Melting Temperatures (T_m), Melting Enthalpies (ΔH), X-ray Crystallinity (x_c), Experimental Triad Distributions, and Enantiomorphic Model Triad Test E of i-PP Samples Prepared with Catalysts of Charts 1 and 2[a]

sample	catalyst/cocatalyst/ carrier[b]	T_p (°C)	M_v[c]	T_m (°C)	ΔH (J/g)	x_c[d]	*mm* %	*mr* %	*rr* %	E[e]
iPP1	**1**/MAO	50	195 700	162	109	0.71	98.54	0.98	0.48	0.98
iPP2	**1**/MAO	60	108 900	157	105	0.69	98.09	1.28	0.63	0.99
iPP3	**1**/MAO/PE	60	120 400	156	93	0.66	97.25	1.83	0.92	1.00
iPP4	**2**/MAO	50	89 000	153	91	0.63	96.90	2.13	0.97	0.91
iPP5	**10**/MAO	70	161 600	150	88	0.60	96.08	2.61	1.31	1.00
iPP6	**9**/MAO	60	184 200	150	88	0.58	96.00	2.67	1.33	1.00
iPP7	**8**/MAO	60	144 500	145	64	0.50	94.34	3.84	1.82	0.95
iPP8	**9**/MAO/PE	60	106 000	140	61	0.48	92.83	4.84	2.33	0.97
iPP9	**7**/MAO/PP	60	202 400	133	44	0.43	89.37	7.04	3.59	1.02
iPP10	**4**/MAO	30	505 800	119	33	0.40	84.12	10.27	5.61	1.09
iPP11	**6**/MAO/PE	60	210 900	116	32	0.39	83.40	10.80	5.80	1.08
iPP12	**3**/MAO	60	166 400	111	22	0.38	78.04	14.44	7.52	1.04
iPP13	**5**/MAO	70	123 400	84	19	0.36	68.20	20.17	11.63	1.15

[a] No or negligible regioerrors (2,1 insertions) could be observed in the ^{13}C NMR spectra of the samples. [b] Some of the MAO-activated complexes were supported on porous polyethylene (PE) or polypropylene (PP) spheres, as described in ref 16. [c] The average molecular masses were obtained from the intrinsic viscosity values according to $[\eta] = K(M_v)^{\alpha}$, with $K = 1.93 \times 10^{-4}$ and $\alpha = 0.74$.[17] [d] From X-ray powder diffraction profiles (Figure 2). [e] $E = 2[rr]/[mr]$.

ligand framework.[12−15] These methylaluminoxane (MAO)-activated zirconocenes produce fully regioregular polypropylenes with relatively high molecular weights, which, depending on the pattern of indene substitution, have largely variable degree of isotacticity and melting temperatures from ca. 80 up to 156 °C.[12−15] The zirconocene structures of this type, selected for the present investigation, are shown in Chart 2. Different crystallization behavior and mechanical properties are expected for these isotactic polypropylene (i-PP) samples.

In this paper we describe the thermal, structural, and mechanical properties of the polypropylenes prepared with the catalysts of Charts 1 and 2, under industrially relevant polymerization conditions, and characterized by different amounts of stereodefects. This report continues our basic studies of polypropylenes of different stereoregularities, aimed at building correlations between polypropylene microstructure and its thermal and mechanical properties.[3−8] The full understanding of the structure−properties relationships will further increase our control over the physical properties of polypropylene and possibly further expand its application range.

Results and Discussion

Preparation and ^{13}C NMR Microstructure Analysis of the Polypropylene Samples. The i-PP samples of the present study are listed in Table 1 (see Experimental Section in the Supporting Information). All samples are fully regioregular, no or negligible amounts of regiomistakes were, indeed, detected in their ^{13}C NMR spectra. They only contain defects of stereoregularity, corresponding to isolated *rr* triads, the amount of *rr* defects depending on the catalyst and polymerization temperature (Table 1). In particular, catalysts **3**−**10** produce i-PP with higher

(12) Nifant'ev, I. E.; Guidotti, S.; Resconi, L.; Laishevtsev, I. P. (Basell, Italy). PCT Int. Appl. WO 01/47939, 2001.
(13) Resconi, L.; Guidotti, S.; Camurati, I.; Nifant'ev, I. E.; Laishevtsev, I. P. *Polym. Mater. Sci. Eng.* **2002**, *87*, 76.
(14) Fritze, C.; Resconi, L.; Schulte, J.; Guidotti, S. (Basell, Italy). PCT Int. Appl. WO 03/00706, 2003.
(15) Nifant'ev, I. E.; Laishevtsev, I. P.; Ivchenko, P. V.; Kashulin, I. A.; Guidotti, S.; Piemontesi, F.; Camurati, I.; Resconi, L.; Klusener, P. A. A.; Rijsemus, J. J. H.; de Kloe, K. P.; Korndorffer, F. M. *Macromol. Chem. Phys.* **2004**, *205*, 2275.

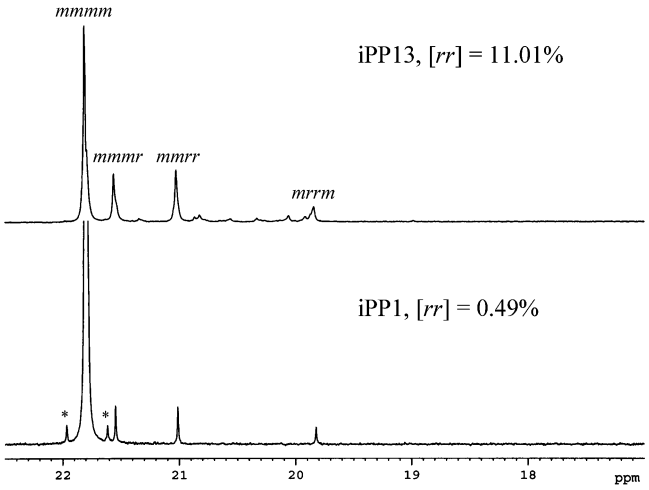

Figure 1. Methyl region resonance of ^{13}C NMR spectra of samples iPP1 (bottom) and iPP13 (top). Peaks marked with * are the $^{13}C-^{13}C$ satellites of the most intense *mmmm* resonance.

amounts of stereodefects compared to catalysts **1**/MAO and **2**/MAO. The more disordered microstructure of the chains produces a more disordered crystalline structure, which in turn imparts an increased flexibility and higher transparency to the polymers. Some of the MAO-activated complexes were also supported on porous polyethylene or polypropylene spheres, as previously described.[16] When not supported, the C_1-symmetric metallocene catalysts **3**−**10** produce polypropylenes of too low crystallinity to grow as powders, but instead, the latter are formed as flexible, tough sheets on the reactor walls or as a spongy mass when the melting point of the polymer is below 100 °C. Support allows obtaining the low-melting i-PP as free flowing spheres, provided that their melting point is above 130 °C. All catalyst syntheses and polymerization results have been described in previous works,[12−14] while the details of the catalysts structure and of polymer microstructures will be reported elsewhere.

Almost all the produced i-PP samples have molecular masses in the range $M_v = (1-2) \times 10^5$. Only samples iPP4 and iPP10 have molecular masses lower than 1×10^5 and much higher than 2×10^5, respectively (Table 1). Since for all the samples sufficiently high values of the molecular mass are obtained, the differences do not influence the physical properties and the crystallization behavior of the samples. The SEC curves show narrow molecular weight distributions, typical of single-center zirconocene catalysts, with polydispersity indices M_w/M_n variable in the range 2−3.

The microstructures of the i-PP samples of Table 1 were determined by solution ^{13}C NMR analysis. The samples are characterized by the presence of different amounts of defects of stereoregularity, corresponding to isolated *rr* triads. The methyl region of ^{13}C NMR spectra of samples iPP1 and iPP13, prepared with **1**/MAO and **5**/MAO, respectively, are presented in Figure 1, as an example. It is apparent that no measurable regioerrors are observed in the ^{13}C NMR spectra. Depending on the catalyst, the amount of *rr* defects changes between 0.5 and 11%, and correspondingly, the samples show melting temperatures variable between 162 and 80 °C (Table 1). The experimental triad distribution and the enantiomorphic model triad test ($E = 2[rr]/[mr]$, $E = 1$ for perfect site control) are reported in the Table 1.

To better understand the catalytic behavior of this class of metallocenes, we performed a statistical modeling on the experimental pentad distribution. As the enantiomorphic model triad test was found to be close to 1 for all samples (Table 1), the experimental pentad distribution was satisfactorily fitted with the simple enantiomorphic site model. The calculated pentad distribution, the probability parameters obtained, and the least-squares values are collected in Table 2, together with the average length of the isotactic sequences ($\langle L_{iso} \rangle = (2[mm]/[mr]) + 2$).

Structural Characterization. All polypropylenes from metallocene catalysts, due to the random distribution of regio- and stereodefects, are characterized by lower crystallinity and lower melting point with respect to the standard i-PP homopolymer melting at about 165 °C. Isotactic polypropylene crystallizes in three different polymorphic forms (α, β, and γ forms),[18] characterized by chains in the 3-fold helical conformation. The crystallization properties of i-PP samples prepared with metallocene catalysts have recently been analyzed.[3−6,19−24] It has been shown that the polymorphic behavior of i-PP, and, in particular, the relative stability of the α and γ forms under common conditions of crystallization, is closely related to the chain microstructure.[3−6,19−24] In particular, metallocene-made i-PP, characterized by chains including different types of microstructural defects (stereodefects and regiodefects), generally crystallizes as a mixture of α and γ forms. The relative content of the two polymorphs depends on the crystallization temperature and the content of defects.[4−6,19−21,24] The formation of the γ form seems to be favored by the presence of stereodefects (mainly *rr* isolated triads),[4−6,21] and/or regiodefects (mainly 2,1 and 3,1 insertions)[19−21] and also by the presence of constitutional defects, like comonomeric units.[23−25]

Crystals of the γ form obtained in these samples always present structural disorder,[5] characterized by defects in the regular packing of bilayers of chains with axes oriented alternatively along two nearly perpendicular directions, typical of γ form.[3−6] In these disordered modifications, bilayers of chains succeed along a crystallographic direction with chain axes either parallel, as in the α form, or perpendicular to each other, as in the γ form.[3] Hence, this disorder produces a local situation of packing typical of the α form, with some adjacent bilayers having parallel chains (α/γ disorder).

Therefore, metallocene i-PP crystallizes in a continuum of disordered modifications intermediate between α and γ forms, the amount of disorder being dependent on the crystallization conditions and on the stereoregularity of the sample.[3−6]

It has recently been shown that also the kind of distribution of defects along the polymer chains influences the polymorphic

(16) Covezzi, M.; Fait, A. (Basell, Italy). PCT Int. Appl. WO 01/44319, 2001.
(17) Moraglio, G.; Gianotti, G.; Bonicelli, U. *Eur. Polym. J.* **1973**, *9*, 693.
(18) Natta, G.; Corradini, P. *Nuovo Cimento Suppl.* **1960**, *15*, 40.
(19) Fischer, D.; Mülhaupt, R. *Macromol. Chem. Phys.* **1994**, *195*, 1433.
(20) Thomann, R.; Wang, C.; Kressler, J.; Mulhaupt, R. *Macromolecules* **1996**, *29*, 8425.
(21) Alamo, R. G.; Kim, M. H.; Galante, M. J.; Isasi, J. R.; Mandelkern, L. *Macromolecules* **1999**, *32*, 4050.
(22) VanderHart, D. L.; Alamo, R. G.; Nyden, M. R.; Kim, M. H.; Mandelkern, L. *Macromolecules* **2000**, *33*, 6078.
(23) Alamo, R. G.; VanderHart, D. L.; Nyden, M. R.; Mandelkern, L. *Macromolecules* **2000**, *33*, 6094.
(24) Thomann, R.; Semke, H.; Maier, R. D.; Thomann, Y.; Scherble, J.; Mülhaupt, R.; Kressler, J. *Polymer* **2001**, *42*, 4597.
(25) Hosier, I. L.; Alamo, R. G.; Esteso, P.; Isasi, G. R.; Mandelkern, L. *Macromolecules* **2003**, *36*, 5623.

Table 2. Calculated Pentad Distributions, Probability Parameters (*b*), Least Square Values for the Enantiomorphic Site Model (LS), and Average Length of Isotactic Sequences $\langle L_{iso} \rangle$[a]

sample	*mmmm* %	*mmmr* %	*rmmr* %	*mmrr* %	*xmrx* %	*rmrm* %	*rrrr* %	*rrrm* %	*mrrm* %	*mm* %	*mr* %	*rr* %	LS	*b*	$\langle L_{iso} \rangle^b$
iPP1	97.55	0.97	0.00	0.97	0.01	0.00	0.00	0.00	0.49	98.52	0.99	0.49	8.57×10^{-1}	0.9950	200
iPP2	96.77	1.27	0.00	1.27	0.02	0.01	0.00	0.01	0.64	98.05	1.30	0.65	8.57×10^{-1}	0.9935	153
iPP3	95.81	1.65	0.01	1.65	0.03	0.01	0.01	0.01	0.82	97.46	1.69	0.85	6.19×10^{-9}	0.9915	117
iPP4	94.72	2.07	0.01	2.07	0.05	0.02	0.01	0.02	1.03	96.80	2.13	1.07	8.57×10^{-3}	0.9892	93
iPP5	93.29	2.61	0.02	2.61	0.07	0.04	0.02	0.04	1.30	95.92	2.72	1.36	1.77×10^{-14}	0.9862	73
iPP6	93.29	2.61	0.02	2.61	0.07	0.04	0.02	0.04	1.31	95.92	2.72	1.36	2.14×10^{-1}	0.9862	72
iPP7	90.03	3.82	0.04	3.82	0.17	0.08	0.04	0.08	1.91	93.89	4.07	2.04	4.46×10^{-5}	0.9792	48
iPP8	87.61	4.70	0.06	4.70	0.26	0.13	0.06	0.13	2.35	92.37	5.08	2.54	3.62×10^{-5}	0.9739	38
iPP9	82.19	6.58	0.14	6.58	0.55	0.27	0.14	0.27	3.29	88.90	7.40	3.70	3.23×10^{-5}	0.9615	26
iPP10	73.91	9.22	0.31	9.22	1.22	0.61	0.31	0.61	4.61	83.43	11.05	5.52	1.25×10^{-4}	0.9413	17
iPP11	72.17	9.73	0.35	9.73	1.40	0.70	0.35	0.70	4.87	82.25	11.83	5.92	1.46×10^{-4}	0.9369	16
iPP12	64.54	11.82	0.59	11.82	2.36	1.18	0.59	1.18	5.91	76.95	15.37	7.68	1.62×10^{-4}	0.9161	12
iPP13	51.00	14.75	1.21	14.75	4.85	2.43	1.21	2.43	7.37	66.97	22.02	11.01	3.02×10^{-4}	0.8740	8

[a] The details of the ^{13}C NMR analysis are reported in the Supporting Information. [b] $\langle L_{iso} \rangle = (2[mm]/[mr]) + 2$

behavior of i-PP and the crystallization of the γ form.[4] In fact, in the case of stereoblock polypropylene, prepared with oscillating metallocene catalysts,[26] the amount of γ form that develops in the melt−crystallization procedures, is much lower than that obtained for i-PP samples having the same overall concentration of defects but prepared with stereorigid metallocene catalysts, which produce a random distribution of defects.[4] This has been explained by considering that in the stereoblock polypropylene most of the defects are segregated in stereoirregular, noncrystallizable blocks, which alternate to more regular isotactic sequences, long enough to crystallize in the α form.[4] This result confirms that the γ form crystallizes when the fully isotactic sequences are very short.[4,5]

These data clearly indicate that, depending on the microstructure of the chains, in particular molecular weight, stereoregularity, and types and distribution of defects, i-PP samples showing different crystal structures and polymorphic behavior may be obtained. It is, therefore, expected that most of the physical properties, which depend on the crystal structure, as the mechanical behavior, are strongly influenced by the chain microstructure.

Detailed studies of the relationships between microstructure, crystal structure, and physical properties of i-PP have been carried out so far only on samples having complex microstructures, containing both regio- and stereoirregularities,[19−21] or in samples consisting in a reactor blend of i-PP fractions having different microstructural features and a large distribution of molecular weights,[4,6,26] or including only stereodefects, but in a small range of concentrations.[5] Therefore, the influence of the presence of a specific microstructural defect on the structure and physical properties of i-PP has not been clarified yet.

Understanding the role played by a single specific defect in affecting the properties of i-PP may allow tailoring different polypropylenes having controlled microstructures and desired physical properties. In particular the issue of the different compatibility of different types of defects in the crystalline lattices of the polymorphic forms of i-PP is of great interest. It has been recently shown that the inclusion of *rr* defects in the crystalline lattice of the γ form allows crystallization of poorly stereoregular polypropylene, inducing development of interesting elastic properties.[3]

(26) Coates, G.; Waymouth, R. M. *Science* **1995**, *267*, 217; Hu, Y.; Krejchi, M. T.; Shah, C. D.; Myers, C. L.; Waymouth, R. M. *Macromolecules* **1998**, *31*, 6908; Witte, P.; Lal, T. K.; Waymouth, R. M. *Organometallics* **1999**, *18*, 4147.

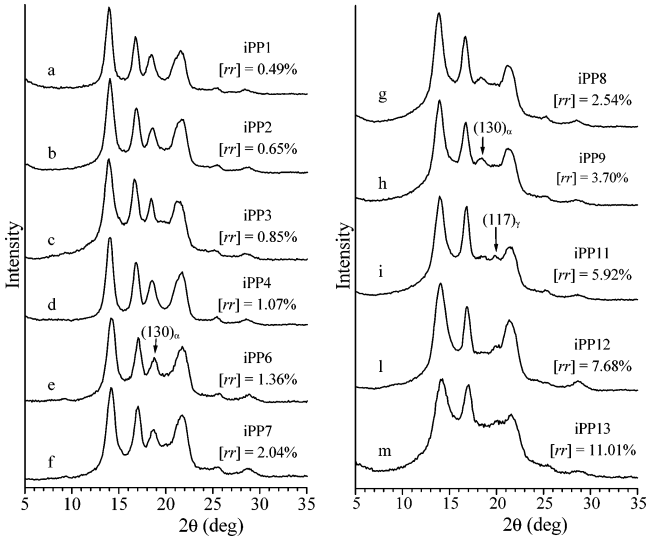

Figure 2. X-ray powder diffraction profiles of as-prepared specimens of i-PP samples of Table 1. The $(130)_\alpha$ reflection of the α form at $2\theta = 18.6°$ and the $(117)_\gamma$ reflection at $2\theta = 20.1°$ of the γ form of i-PP are indicated.

As discussed above, using the catalysts of Charts 1 and 2, a fine-tuning of the microstructure of i-PP chains has been achieved (Table 1). A parallel analysis of the structure, polymorphic behavior, and mechanical properties of the corresponding produced i-PP samples, containing only one type of microstructural defect (isolated *rr* triads), may allow building correlations among the amount of *rr* defect, the crystal structure, and the mechanical properties.

The X-ray powder diffraction profiles of as-prepared specimens of the i-PP samples of Table 1 are reported in the Figure 2. The more stereoregular samples, up to content of *rr* defect of 2%, are basically crystallized in the α form, as indicated by the presence of the $(130)_\alpha$ reflection at $2\theta = 18.6°$ of the α form[18] and the absence of the $(117)_\gamma$ reflection of the γ form at $2\theta = 20.1°$ in the X-ray powder diffraction profiles a−f of Figure 2. Samples containing higher concentration of *rr* defects are crystallized in α/γ disordered modifications of the γ form, as indicated by the low intensity of both $(130)_\alpha$ and $(117)_\gamma$ reflections at $2\theta = 18.6$ and 20.1°, respectively,[3−5] in the diffraction profiles g−i of Figure 2. In these disordered modifications, bilayers of chains succeed along a crystallographic direction with chain axes either parallel, as in the α form, or perpendicular to each other, as in the γ form.[3] The amount of disorder increases with increasing concentration of

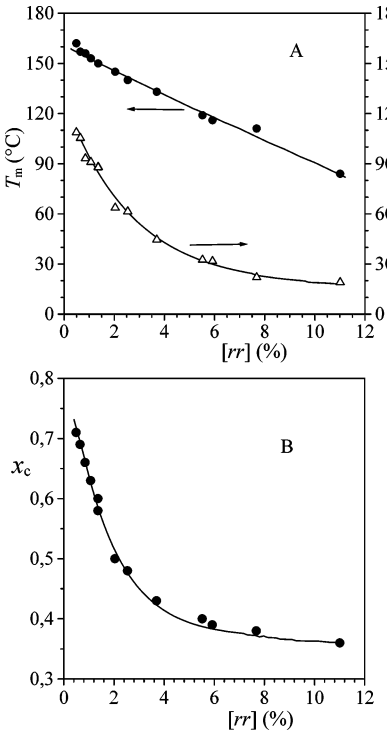

Figure 3. Melting temperatures and enthalpies, evaluated from DSC scans at heating rate of 10 °C/min (A), and X-ray indices of crystallinity (B) of i-PP samples of Table 1 as a function of the concentration of *rr* defects.

stereodefects, as indicated by the absence of both $(130)_\alpha$ and $(117)_\gamma$ reflections in the X-ray diffraction profiles l and m of Figure 2.

The unique crystallization mode of metallocene-made polypropylene in a continuum of disordered modifications intermediate between α and γ forms[3,5] allows maintenance of crystallinity even in poorly isotactic samples, containing high concentration of *rr* defects. In particular, it has recently been shown that *rr* defects can be easily tolerated at low cost of conformational and packing energy in the crystal lattices of the α/γ disordered modifications.[3,5] The inclusion of *rr* defects gives a possible explanation of the development of crystallinity in i-PP samples having very low stereoregularity.[3]

The melting temperatures, enthapies, and the X-ray index of crystallinity of the as-prepared samples are reported in Table 1 and in Figure 3 as a function of concentration of *rr* defects. It is apparent that the melting temperature and the crystallinity of the samples decrease with increasing concentration of *rr* defects, indicating that the physical properties of i-PP can be modulated through the choice of the catalyst structure.

Samples of Table 1 have been isothermally crystallized from the melt at different crystallization temperatures and analyzed by X-ray diffraction. The X-ray diffraction profiles of melt-crystallized specimens of four samples are reported in Figure 4, as examples. The diffraction profiles of the as-prepared samples (already shown in Figure 1) are also reported in Figure 4 (profiles a) for comparison.

All the samples crystallize from the melt in mixtures of the α and γ forms, the fraction of γ form being dependent on the crystallization temperature and the concentration of *rr* defects. The diffraction profiles of Figure 4 present, indeed, both $(130)_\alpha$ and $(117)_\gamma$ reflections, and the relative intensity of the $(117)_\gamma$ reflection of the γ form at $2\theta = 20.1°$ increases with increasing crystallization temperature and with increasing concentration of *rr* defects.

The relative amount of the γ form with respect to the α form, f_γ, evaluated from the intensity of the $(117)_\gamma$ reflection, for the various samples is reported in Figure 5 as a function of the crystallization temperature. As already observed in the literature,[4−6,19−25] for each sample the content of γ form increases with increasing crystallization temperature, and a maximum amount is obtained at temperatures that depend on the concentration of *rr* defect. Moreover, the content of the γ form increases with increasing concentration of *rr* defects. In particular, the more stereoirregular sample iPP13, initially in disordered α/γ modification (profile *a* of Figure 4D), crystallizes from the melt totally in the γ form, as indicated by the high intensity of the $(117)_\gamma$ reflection of the γ form at $2\theta = 20.1°$ and the absence of the $(130)_\alpha$ reflection of the α form at $2\theta = 18.6°$, at any crystallization temperature in the diffraction profiles b−f of Figure 4D.

Curves of the amount of γ form as a function of the crystallization temperature similar to those of Figure 5 have already been reported and discussed in the literature for different samples of i-PP prepared with different metallocene catalysts.[4−6,19−24] However, these samples were characterized by more complex microstructures, containing different types of defects (stereo- and regiodefects); therefore, no simple relationships between the content of defects and polymorphic behavior of i-PP have been found. The samples of Figures 4 and 5 are instead characterized by a very simple microstructure, because the chains contain only *rr* defects in a large range of concentration. These data clarify the effect of *rr* defects on the polymorphic behavior of i-PP, as inducing the crystallization of the γ form. Most of the *rr* defects can be easily tolerated at low cost of conformational and packing energy in the crystal lattices of γ form and of the α/γ disordered modifications.[3,5] As discussed for the as-prepared samples, the inclusion of *rr* defects induces the crystallization of the γ form and of disordered modifications intermediate between α and γ forms of i-PP[3,5] and gives a possible explanation for the development of crystallinity in i-PP samples having very low stereoregularity.[3]

Therefore, the data of Figures 4 and 5 indicate that the relative stability of α and γ forms of i-PP is related to the concentration of defects of stereoregularity and, hence, to the average length of the fully isotactic sequences comprised between two successive interruptions. The γ form is favored when the regular isotactic sequences are short. As discussed above, for i-PP samples of Table 1, the distribution of defects (only isolated *rr* triads) along the polymer chains is random; hence, the average length of the fully isotactic sequences, $\langle L_{iso} \rangle$, is inversely proportional to the content of *rr* errors and can be easily evaluated from the ^{13}C NMR data, as $\langle L_{iso} \rangle = (2[mm]/[mr]) + 2$ (Table 2).

The maximum amount of the γ form that crystallizes upon the melt−crystallization procedures, $f_\gamma(\max)$, for the various i-PP samples is reported in Figure 6 as a function of the average length of the fully isotactic sequences $\langle L_{iso} \rangle$. It is apparent that the maximum amount of γ form that can be obtained is roughly linear with the average length of isotactic sequences $\langle L_{iso} \rangle$, at least in the range of $\langle L_{iso} \rangle = 15-170$ monomeric units. For the most isotactic samples, with higher lengths of isotactic sequences, $\langle L_{iso} \rangle = 190-200$ monomeric units, and *rr* content

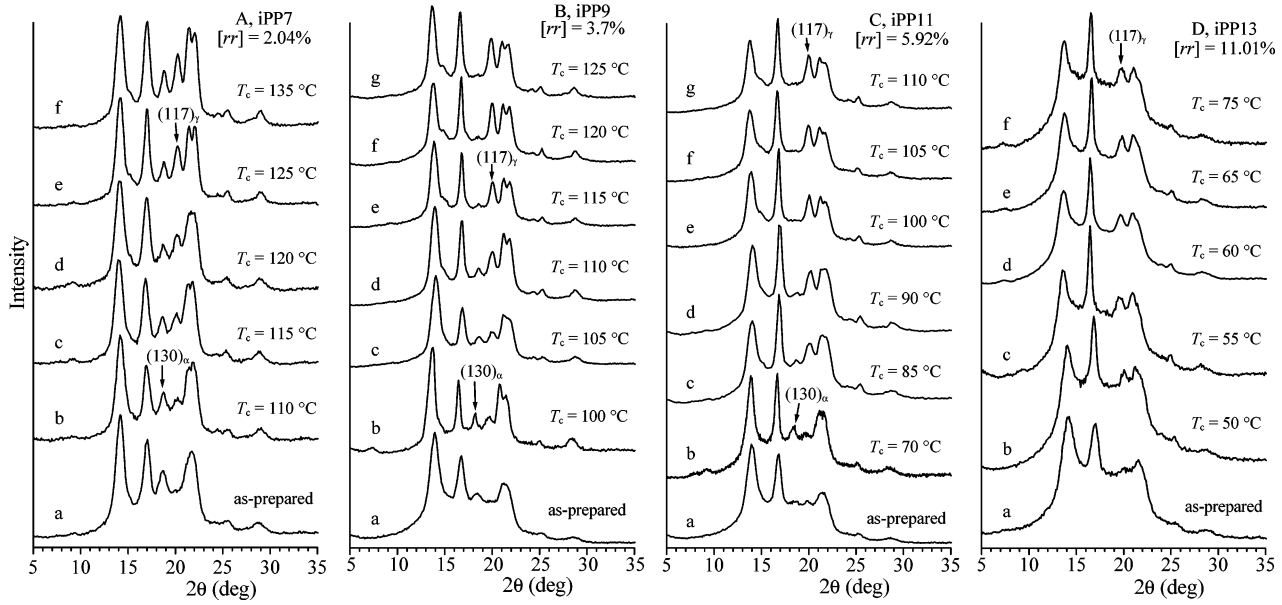

Figure 4. X-ray powder diffraction profiles of some i-PP samples of Table 1 isothermally crystallized from the melt at the indicated temperatures. The $(130)_\alpha$ reflection of the α form at $2\theta = 18.6°$ and the $(117)_\gamma$ reflections of the γ form at $2\theta = 20.1°$ are indicated.

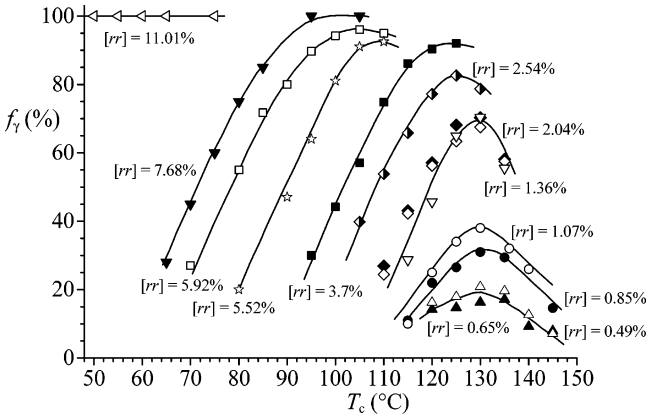

Figure 5. Relative content of γ form, f_γ, in the samples of i-PP isothermally crystallized from the melt, as a function of the crystallization temperature T_c: (△) sample iPP1, [*rr*] = 0.49%; (▲) sample iPP2, [*rr*] = 0.65%; (●) sample iPP3, [*rr*] = 0.85%; (○) sample iPP4, [*rr*] = 1.07%; (▽) sample iPP5, [*rr*] = 1.36%; (◆) sample iPP6, [*rr*] = 1.36%; (◇) sample iPP7, [*rr*] = 2.04%; (half-filled diamond) sample iPP8, [*rr*] = 2.54%; (■) sample iPP9, [*rr*] = 3.70%; (☆) sample iPP10, [*rr*] = 5.52%; (□) sample iPP11, [*rr*] = 5.92%; (▼) sample iPP12, [*rr*] = 7.68%; (open, tilted triangle) sample iPP13, [*rr*] = 11.01%.

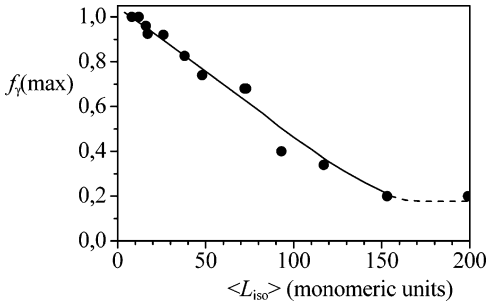

Figure 6. Maximum amount of γ form, f_γ(max), obtained upon melt−crystallization procedures, for the various samples of i-PP of Table 1, as a function of the average length of fully isotactic sequences $\langle L_{iso}\rangle$. The deviation from the linear relationship for values of $\langle L_{iso}\rangle$ higher than 170−180 monomeric units is indicated with the dashed line.

lower than 0.6% (Table 2), the amount of γ form approaches a limit constant value of nearly 15−20%. Hence, the relationship of Figure 6 deviates from the linear function for highly isotactic samples and high values of the average isotactic sequences length. This is due to the fact that in the case of metallocene-made i-PP the amount of γ form is never reduced to zero, even for very low concentration of *rr* defects, as instead occurs for samples prepared with Ziegler−Natta catalysts. In fact, because of the random distribution of defects in chains of i-PP samples prepared with single-center metallocene catalysts, even a small amount of defects reduces the length of the regular isotactic sequences, inducing the crystallization of the γ form.

In the case of i-PP samples prepared with heterogeneous Ziegler−Natta catalysts, instead, the majority of the defects may be segregated in a small fraction of poorly crystallizable macromolecules, so that much longer fully isotactic sequences can be produced, leading to the crystallization of the α form.[7]

It is worth noting that amounts of γ form lower than the limit value of 15−20% are obtained even for samples with high contents of *rr* defects when the samples are crystallized by quenching the melt to room temperature at cooling rates higher than 40 °C/min.

In i-PP samples having different microstructures, containing different types of defects of stereoregularity and regioregularity, a nonlinear relationship has been obtained and reported in the literature.[4] It was shown, indeed, that the maximum amount of γ form that can be obtained for various i-PP samples also containing regioerrors[21] is linear with the logarithm of $\langle L_{iso}\rangle$, which was defined as inversely related to total amount ϵ of regio- and stereodefects, $\langle L_{iso}\rangle \approx 1/\epsilon$.[4]

This indicates that different types of microstructural defects may induce a different crystallization behavior of i-PP. The data of Figure 6 obtained for the samples of Table 1, containing only *rr* defects, allow discriminating the single effect of *rr* defects on the polymorphic behavior of metallocene-made i-PP. The increase of concentration of *rr* defects reduces the length of regular isotactic sequences and produce a linear increasing of the amount of γ form.

A low conformational energy model of a chain of i-PP containing *rr* configurational defects, able to pack in the

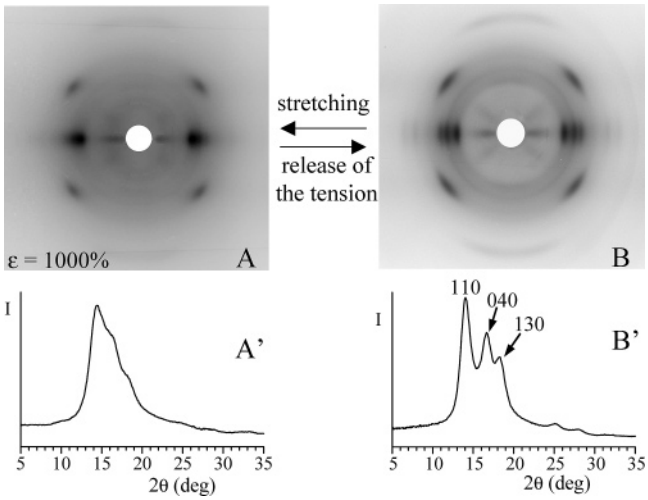

Figure 7. X-ray fiber diffraction patterns (A, B) and corresponding profiles read along the equatorial lines (A′, B′), of fibers of the sample iPP13 with [*rr*] = 11.01%, obtained by stretching compression-molded films at 1000% elongation, keeping the fiber under tension (A, A′), and removing the tension (B, B′). The 110, 040, and 130 reflections at $2\theta = 14$, 17, and 18.6°, respectively, typical of the α form of i-PP, are indicated. The fiber in A is in the mesomorphic form, whereas the fiber in B is in the crystalline α form.

structure of γ form and/or in α/γ disordered modifications of i-PP, has been recently proposed.[3] The inclusion of *rr* defects in the crystals of γ form plays an important role in defining the linear relationship of Figure 6 and introduces a possible mechanism inducing, in poorly stereoregular i-PP samples, the observed tendency to give rise to intermediate modifications between the α and γ forms.[3−5] As will be discussed in the next section, the linear relationship between the content of *rr* defects and crystallization behavior reflects the strong influence of *rr* defects on the mechanical properties of i-PP.

Oriented fibers of the i-PP samples of Table 1 have been obtained by stretching at room temperature at a drawing rate of 10 mm/min compression-molded samples. All samples of Table 1 can be drawn at room temperature, regardless of the concentration of *rr* defects. For all samples the easy deformation at high values of the draw ratio produces transformation of the crystals of α or γ forms, present in the unstretched compression molded films, into the disordered mesomorphic form of i-PP. We recall that the mesomorphic form of i-PP is generally obtained by rapidly quenching the melt to very low temperatures and is characterized by chains in the ordered 3-fold helical conformation but a high degree of disorder in the lateral packing of chains.[27]

The X-ray fiber diffraction pattern and the corresponding intensity profile read along the equatorial line of the sample iPP13 with content of *rr* defects of 11.01%, stretched at 1000% deformation and keeping the fiber under tension, are reported in Figure 7A and A′, respectively. It is apparent that fibers in the mesomorphic form are obtained, as indicated by the presence of the broad haloes on the equator in the range $2\theta = 14-16°$ and on the first layer line (Figure 7A).[27] Similar patterns have been obtained for the other samples of Table 1. Depending on the concentration of *rr* defects, compression-molded unstretched films are in α or γ forms or in mixture of α and γ forms (Figure 4), which both transform into the mesomorphic form by stretching at high deformation.

The X-ray diffraction pattern and the corresponding equatorial profile of fibers of the sample iPP13 stretched at 1000% elongation (Figure 7A,A′), after releasing the tension, are reported in Figure 7B and B′, respectively. It is apparent that the mesomorphic form (Figure 7A) transforms into the α form of i-PP upon releasing the tension, as indicated by the presence of the 110, 040, and 130 reflections at $2\theta = 14$, 17, and 18.6°, typical of the crystalline α form, in the diffraction pattern of Figure 7B,B′. This transformation is reversible upon successive stretching and relaxing cycles. The crystalline α form transforms by stretching into the disordered mesomorphic form, which, in turn, transforms into the α form by releasing the tension (Figure 7). Similar behavior has been observed for the sample iPP12 with [*rr*] = 7.68%.

It is worth noting that the transformation of the mesomorphic disordered form into the α form corresponds to an increase of crystalline order. The crystallization upon removing the tension in stretched fibers is not common in polymers.

In the case of the more regular sample iPP11 with [*rr*] = 5.92%, this polymorphic transition is no longer reversible, i.e., the mesomorphic form obtained by stretching at high deformation does not transform into the α form by releasing the tension. For the more crystalline samples with concentration of *rr* defects lower than 3−4%, the α form crystals present in the unoriented compression-molded films also transforms into the mesomorphic form by stretching, but a low degree of orientation is obtained due to the lower degree of deformation that can be achieved at room temperature. Also in these samples the mesomorphic form does not transform into the α form upon removing the tension.

Mechanical Properties. In this section preliminary results of the analysis of the mechanical properties of i-PP samples of Table 1 are reported. The effect of the presence of *rr stereo*-defects on the mechanical properties of i-PP and relationships between the concentration of defects, the crystal structure, and the mechanical properties have been analyzed.

The stress−strain curves of compression-molded films of i-PP samples of Table 1 having different concentrations of *rr* defects are reported in Figure 8. The values of Young modulus decreases with increasing concentration of *rr* defects and decreasing crystallinity, from nearly 200 MPa for the sample iPP1 to nearly 19 MPa for the sample iPP13. The values of deformation at yield point and at break instead increase with increasing concentration of defects. The lower values of deformation at break observed for the samples iPP8 and iPP12 are probably due to the lower values of molecular weight (Table 1). As expected, parallel to the decrease of the values of the modulus, a decrease of the stress at yielding with increasing concentration of defects is observed.

These data indicate that the more crystalline samples (x_c = 60−70%), up to a concentration of *rr* defects of 2−3%, show similar ductility and toughness, whereas a strong increase of ductility and toughness is observed for higher contents of *rr* defects and lower crystallinity (x_c = 40−50%).

The values of stress at break (tensile strength) are nearly constant for the more crystalline samples (up to *rr* content of 3−4%) and then decrease for a further increase of concentration of defects (up to [*rr*] = 5.9%), according to the decrease of crystallinity. Surprisingly, the tensile strength strongly increases

(27) Guerra, G.; Petraccone, V.; De Rosa, C.; Corradini, P. *Makromol. Chem., Rapid Commun.* **1985**, *6*, 573. Corradini, P.; Petraccone, V.; De Rosa, C.; Guerra, G. *Macromolecules* **1986**, *19*, 2699.

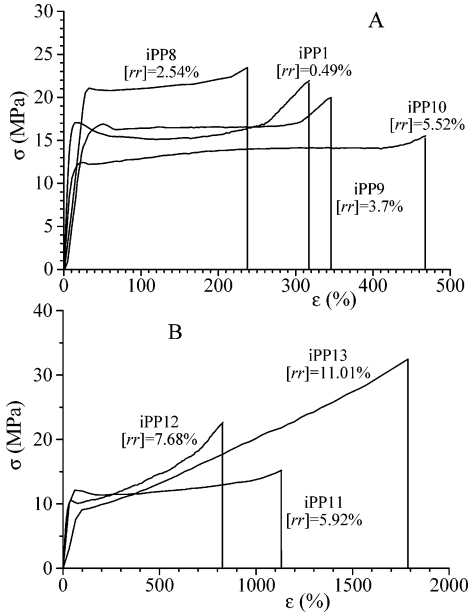

Figure 8. Stress−strain curves of unoriented compression-molded films of some i-PP samples of Table 1. The values of the mechanical parameters, elastic modulus, stress and strain at break, stress and strain at the yield point, and tension set and elastic recovery after breaking, are reported on the Internet as Supporting Information.

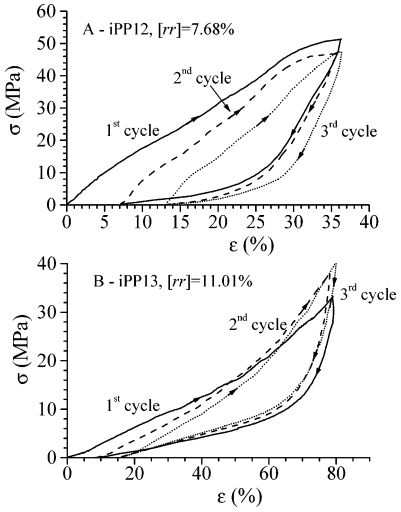

Figure 9. Stress−strain hysteresis cycles recorded at room temperature, composed of stretching and relaxation (at controlled rate) steps according to the direction of the arrows, for stress-relaxed fibers of the samples iPP12 (A) and iPP13 (B). The stress-relaxed fibers have been prepared by stretching compression-molded films, of initial length L_0, up to 500% elongation (final length $L_f = 6L_0$) and then removing the tension. In the hysteresis cycles the stretching steps are performed by stretching the fibers up to final length $L_f = 6L_0$. Continuous lines, first cycle; dashed lines, second cycle; dotted lines, third and successive cycles.

for a further increase of the amounts of *rr* defects (Figure 8B). The lowest crystalline sample, with the highest concentration of defects (sample iPP13 with [*rr*] = 11% and $x_c = 42\%$), shows strong strain hardening at high deformation (Figure 8B) with values of the tensile strength (32 MPa) higher than those of the more crystalline samples (20−23 MPa).

The data of Figure 8 indicate that samples of i-PP containing a low concentration of *rr* defects (up to [*rr*] = 4−5%, Figure 8A) show the typical behavior of stiff-plastic materials, with high values of the elastic modulus (Figure 8A). Nevertheless, these samples can be stretched at room temperature up to remarkable values of the strain (400−500%, Figure 8A). Samples with a higher concentration of *rr* defects ([*rr*] = 5.92%) present similar behavior with slightly lower strength but much higher deformation at break ($\epsilon_b \approx 1200\%$, Figure 8B). This indicates that these samples ([*rr*] = 5−6% and melting temperatures around 115 °C, for instance the sample iPP11) behave as highly flexible thermoplastic materials.

Samples with the highest concentrations of *rr* defects ([*rr*] = 7−11%) show elastomeric properties. The samples iPP12 and iPP13 show, indeed, good elastic recovery after breaking. Moreover, their stress−strain curves present the typical shape of elastomeric materials (Figure 8B), showing high values of deformation at break and strain-hardening at high deformation.

In these materials the elastic properties are associated with remarkable values of the modulus, nearly 20−30 MPa. This is due to the fact that these samples are crystalline notwithstanding the low stereoregularity. As discussed in the previous section, these samples crystallize in the γ form of i-PP or in α/γ disordered intermediate modifications, thanks to the inclusion of most of the *rr* stereodefects.

The formation of small crystalline domains induces elastomeric properties, since crystals act as physical cross-links in the amorphous matrix, producing the elastomeric network. The presence of crystallinity gives high values of the strength, so that interesting thermoplastic elastomers with remarkable values of the modulus and tensile strength are obtained. In particular, the more irregular sample iPP13 ([*rr*] = 11%), which can be stretched at very high deformation (up to 1800%, Figure 8B), presents a strong increase of the stress at high deformation (strain hardening). The value of the tensile strength (stress at break = 32 MPa, Figure 8B) is, indeed, even higher than that observed in the more stereoregular and crystalline samples having [*rr*] < 5% (Figure 8A). This behavior is unusual for elastomers, which generally show values of the tensile strength much lower than those of crystalline thermoplastic materials.

The elastic properties of the samples iPP12 and iPP13 have also been studied in oriented fibers prepared by stretching compression-molded films of initial length L_0 up to 500% elongation (final length $L_f = 6L_0$) and then removing the tension. To quantify the elastic behavior, hysteresis cycles have been recorded at room temperature. The hysteresis cycles, composed of the stress−strain curves measured during the stretching of fibers of samples iPP12 and iPP13, immediately followed by the curves measured during the relaxation at controlled rate, are reported in Figure 9. In these cycles, stress-relaxed oriented fibers of the new initial length L_r are stretched up to the final length $L_f = 6L_0$, with L_0 the initial length of the unoriented film. Successive hysteresis cycles, measured after the third one, are all nearly coincident, indicating a tension set close to zero and a perfect elastic recovery.

The outstanding properties of the elastomeric samples iPP12 and iPP13 are probably related to the increase of crystallinity during stretching and the structural transitions occurring during stretching. As shown by the structural analysis discussed in the previous section, during stretching of these samples the γ form present in the unstretched compression-molded film transforms into the mesomorphic form of i-PP, which, in turn, transforms into the crystalline α form upon releasing the tension (Figure 7). Correspondingly, a recovery of the dimension is observed (Figure 9). These data indicates that the elastic behavior of

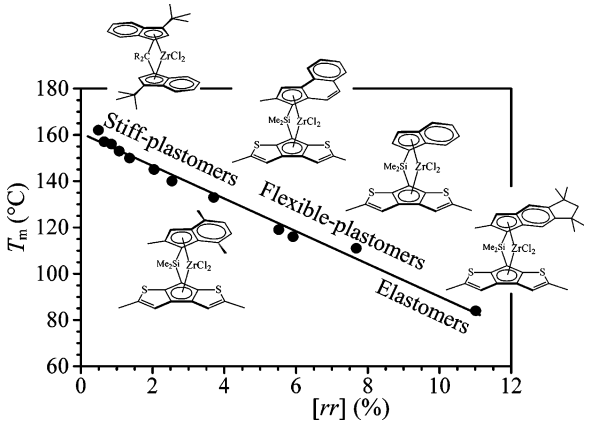

Figure 10. Classification of i-PP samples as stiff-plastic materials, flexible-plastic materials, and thermoplastic elastomers depending on melting temperature and concentration of *rr* defects of stereoregularity.

fibers of samples iPP12 and iPP13 is associated with a reversible polymorphic transition between the mesomorphic form and the α form of i-PP. In particular, the elastic recovery is associated with the crystallization of the mesomorphic form into the α form upon releasing the tension. It is worth noting that the crystallization upon removing the tension in stretched fibers is not common for elastomeric materials. In the case of common elastomers, like natural rubber, crystallization occurs by stretching, and crystals melt upon removing the tension.

The data of Figure 8 have shown that the more stereoregular and crystalline sample iPP11, with content of *rr* defects of 5.92%, does not show elastic behavior but behaves as a highly flexible thermoplastic material. For this flexible sample, no reversible transition is observed during stretching and relaxation. The mesomorphic form obtained by stretching at high deformation does not transform into the α form upon removing the tension. This indicates that, for these metallocene-made i-PP, only when the sample experiences elastic recovery is the polymorphic transition between mesomorphic and α forms observed.

The analysis of the crystallization behavior and mechanical properties of i-PP samples having different concentration of *rr* defects clearly demonstrates that, depending on the amount of *rr* defects, different physical properties are obtained. Samples with low concentration of *rr* defects, up to 3−4%, present high melting temperatures, in the range 160−130 °C, and behave as stiff-plastic materials (Figure 10); samples with higher *rr* content, in the range 5−6% and melting temperatures around 115−120 °C, are highly flexible thermoplastic materials, and, finally, samples with a concentration of *rr* defects in the range 7−11% and melting temperature in the range 80−110 °C are thermoplastic elastomers with high strength (Figure 10).

Conclusions

Samples of i-PP with controlled microstructure have been obtained with catalysts shown in Charts 1 and 2. Depending on the structure of the catalysts, in particular the substitution on the indenyl ligand, samples with similar molecular weights and variable stereoregularity have been obtained. The samples are highly regioregular and contain only *rr* defects of stereoregularity in a large range of concentration, with melting temperatures ranging between 160 and 80 °C. The simple microstructure of the polymer chains has allowed understanding the effect of the presence of *rr* defects on the crystallization behavior and physical properties of i-PP.

The samples crystallize from the melt in mixtures of α and γ forms. The content of the γ form increases with increasing crystallization temperature and concentration of *rr* defects. The presence of *rr* defects induces crystallization of the γ form and of disordered modifications intermediate between α and γ forms. Most of the *rr* defects can be easily tolerated in the crystal lattice of the γ form and of the α/γ disordered modifications, inducing crystallization of the γ form and giving a possible explanation for the crystallization of low stereoregular i-PP samples and, as a consequence, for the development of elastomeric properties.

Because of the simple microstructure and the random distribution of *rr* defects along the polymer chains, the concentration of *rr* defect is strictly related to the average length of regular isotactic sequences. The higher the content of *rr* defects, the shorter the length of isotactic sequences and the higher the amount of γ form which crystallizes from the melt. A linear relationship between a structural parameter, the amount of crystallized γ form, and a microstructural parameter, the average length of isotactic sequences, has been found.

The analysis of mechanical properties has shown that *rr* defects also influence the physical properties of i-PP. Different concentrations of *rr* defects induce different crystallization behavior and different physical properties. Samples with a low concentration of *rr* defects, up to 3−4%, present high melting temperatures, in the range 160−130 °C, and behave as stiff-plastic materials. Sample with higher *rr* content, in the range 5−6%, and melting temperatures around 115−120 °C are highly flexible thermoplastic materials, showing very high deformation at break. Samples with concentration of *rr* defects in the range 7−11% and melting temperature in the range 80−110 °C are thermoplastic elastomers with high strength. Properties such as high flexibility and elasticity are not accessible with commercial polypropylene produced with traditional Ziegler−Natta catalysts.

The outstanding properties of the elastomeric samples are related to structural transitions occurring during stretching. For the elastomeric samples the γ form present in the unstretched compression-molded film transforms by stretching into the mesomorphic form, which transforms into the crystalline α form upon releasing the tension. Correspondingly, a recovery of the initial dimension of the sample is observed. The crystallization of the mesomorphic form into the α form upon releasing the tension is not observed in the case of flexible or stiff-plastic samples, which do not show elastic behavior. These data indicates that the elastic behavior of less crystalline and stereoregular samples is associated with a reversible polymorphic transition between the mesomorphic form and the α form of i-PP.

These results indicate that a detailed understanding of the effects of the microstructure of the chain molecules on the crystal structure and properties of polypropylene has allowed the tailored design of new polymerization catalysts for producing polypropylenes having controlled microstructures and controlled desired properties, not accessible with commercial polypropylene produced with traditional Ziegler−Natta catalysts, intermediate between those of stiff-plastic and elastomeric materials.

Acknowledgment. Financial supports from Basell Polyolefins (Ferrara, Italy) and from the "Ministero dell'Istruzione, dell'Università e della Ricerca" (PRIN 2002 and Cluster C26

projects) are gratefully acknowledged. We thank Paolo Ferrari and Marina Malusardi for the preliminary characterization of the flexible polypropylene samples described in this work.

Supporting Information Available: Experimental section, details of ^{13}C NMR analysis, and mechanical properties evaluated from the analysis of the stress−strain tests. This material is available free of charge via the Internet at http://pubs.acs.org.

JA045684F